Scientific Research Publishing

Open Journal of Earthquake Research, 2017, 6, 191-203
http://www.scirp.org/journal/ojer
ISSN Online: 2169-9631
ISSN Print: 2169-9623

Unusual Change in Critical Frequency of F_2 Layer during and Prior to Earthquakes

Soujan Ghosh[1], Sudipta Sasmal[1], Subrata Kumar Midya[1,2], Sandip K. Chakrabarti[1,3]

[1]Indian Centre for Space Physics, Kolkata, India
[2]Department of Atmospheric Sciences, Calcutta University, Kolkata, India
[3]S. N. Bose National Centre for Basic Sciences, Kolkata, India
Email: soujanghosh89@gmail.com, meet2ss25@gmail.com, drskm06@yahoo.co.in, sandipchakrabarti9@gmail.com

How to cite this paper: Ghosh, S., Sasmal, S., Midya, S.K. and Chakrabarti, S.K. (2017) Unusual Change in Critical Frequency of F_2 Layer during and Prior to Earthquakes. *Open Journal of Earthquake Research*, **6**, 191-203.
https://doi.org/10.4236/ojer.2017.64012

Received: June 15, 2017
Accepted: October 16, 2017
Published: October 19, 2017

Copyright © 2017 by authors and Scientific Research Publishing Inc.
This work is licensed under the Creative Commons Attribution International License (CC BY 4.0).
http://creativecommons.org/licenses/by/4.0/

Open Access

Abstract

The unusualness in the critical frequency of different layers of earth's ionosphere is commensurate to be associated with seismic events. We present study of critical frequency of F_2 layer (denoted as f_0F_2) during some major earthquakes in South American region. We use the semi-empirical Barbier's theorem of air-glow and define a parameter using the critical frequency and virtual height of F_2 layer and named it as "F Parameter". To investigate the variation of this parameter, we consider five large earthquakes in the junction of Nazca plate and South American plate having magnitude greater than M > 6.5 and study the temporal variation of F parameter during these earthquakes. The F Parameter is measured using the ionograms as recorded from the Ionosonde in Jicamarca Radio Observatory (lat. 11.95˚S, long 76.87˚W) in Chile which lies within the earthquake preparation zones of these five earthquakes. We examine the F Parameter within a span of ±15 days during earthquakes and observed significant change in the evaluated F Parameter in 12 to 3 days prior to the earthquakes. The increment is over +3σ from the normal variation. We also observe significant changes during aftershock events. The solar geomagnetic indices were found to be low which ensures that these anomalies in F Parameter are due to seismic events.

Keywords

Earthquake Early Warning, Wave Propagation, Earthquake Interaction, Forecasting and Prediction, Ionosphere/Atmosphere Interactions, Electrical Properties

1. Introduction

This understanding of seismicity is a vast, complicated, anisotropic and multi

parametric problem. Predictions of earthquakes from perceived precursory phenomena with accurate specification of time, location and magnitude of a future earthquake with sufficient precision is therefore not very easy. It is well recognized that electromagnetic wave propagation technique through earth-ionosphere waveguide could be an important tool to predict occurrences of seismic hazards. The mechanism of seismicity can create a significant thermal, mechanical and electrical perturbation in ionospheric layers through the so-called Lithosphere-Atmosphere-Ionosphere Coupling (LAIC). Thus any physical or chemical changes resulting from such a coupling can be used as a precursory tool for seismic hazards.

Ionosphere is divided in mainly three distinct layers, namely, D, E and F. F is also divided in two sub layers, namely, F_1 and F_2. The behavior of F_2 layer is described in terms of the extent of its departure from that of a hypothetical Chapman layer. The departure can be termed as an "anomaly". Geographical anomaly, Diurnal anomaly, Seasonal anomaly, winter anomaly are some of such anomalies observed usually in the experimental measurement of Critical frequency of F_2 layer. The Critical frequency is the highest frequency which could be reflected from ionosphere. Above this frequency, the radio wave penetrates into the upper ionosphere. The critical frequency of F_2 layer is denoted by f_0F_2. When a radio wave is reflected from a perfect reflector, it is likely to be reflected from a point. But in reality the signal is continuously bent or refracted as it travels through ionosphere, since the reflection and penetration both occurs simultaneously till a height is reached where the residual ray is totally reflected. However, though the path is bent gradually, one can conceive that the incident and reflected rays, when extrapolated, meet at a point. This height could be called the virtual reflection height. The virtual height of an ionized atmospheric layer is measured by the time interval between the transmission of a radio signal and the receipt of the return of its echo.

The existence of a phenomenon called "airglow" was probably discovered before 1800. Yntema [1] was the first person to photometrically establish the phenomenon of airglow which he termed as Earthlight. Following a suggestion of Otto Struve, Elvey [2] introduced the name airglow for the first time. From the basic physics of airglow, related chemical kinetics and excitation mechanism and above all, the ionospheric physics and chemistry, it is obvious that there exists a direct relationship, either of complex or of straightforward nature between ionospheric parameters and airglow emissions. The well-known Barbier formula establishes a direct relationship between the airglow intensity and the critical frequency of the F_2 layer. The variable part of this formula deals with the critical frequency and the virtual reflection height of F layer. The airglow intensity variation depends on the charge densities and type of ions which recombines to emit the radiation. As a whole, the critical frequency is associated with the charge density profile of the ionospheric layers. So can be used as a tool to study the variabilities of the charge density profiles. LAIC mechanism predicts anomalous changes of charge density profile before seismic events.

Ionospheric disturbance associated with seismic activities has been largely studied since the Great Alaska Earthquake in March 27, 1964 [3]-[30]. Correlations of seismicity with anomaly in F-layer were achieved using different methodologies from spectral analysis [31], satellite observation [32], equatorial ionization anomaly [33], etc. The first publications deal with ionospheric characteristics variations as seismic precursors were Antselevich [34] study of the variations of f_0E parameter before the Tashkent earthquake 1966. The peak electron density in the F_2 layer appears to be one of the most sensitive parameters connected to seismic activity. Spatial and Temporal variation of electron concentration based on topside ionosonde data during seismic events was done by Pulinets *et al.* [35]. Several studies were carried out regarding the f_0F_2 variation by Gaivoronskaya & Zelenova [36]; Dupuev & Zelenova [37]; Chuo *et al.* [38]; Pulinets *et al.* [39] [40]; Liu *et al.* [41]; Silina *et al.* [42]; Pulinets & Legen'ka [43]; Rios *et al.* [44]; Pulinets & Boyarchuk [16]; Hobara & Parrot [45]; Liperovskaya *et al.* [46].

In this paper, we consider five different earthquakes from South American region near Peru and Chile. We compute a variable parameter from Barbier theorem using the (f_0F_2) and virtual height profile and study this parameter for a duration of ±15 days around those five earthquakes. The plan of the paper is as following: in the next Section, we explain the methodology and data analysis; in Section 3, we present our results; and in Section 4, we draw our conclusion.

2. Data and Methodologies

In our entire analysis, we gathered the Ionosonde data from Jicamarca station from http://digisonde.com. In **Figure 1**, we present schematic diagram of radio wave propagation technique to indicate the reflection height and critical frequency.

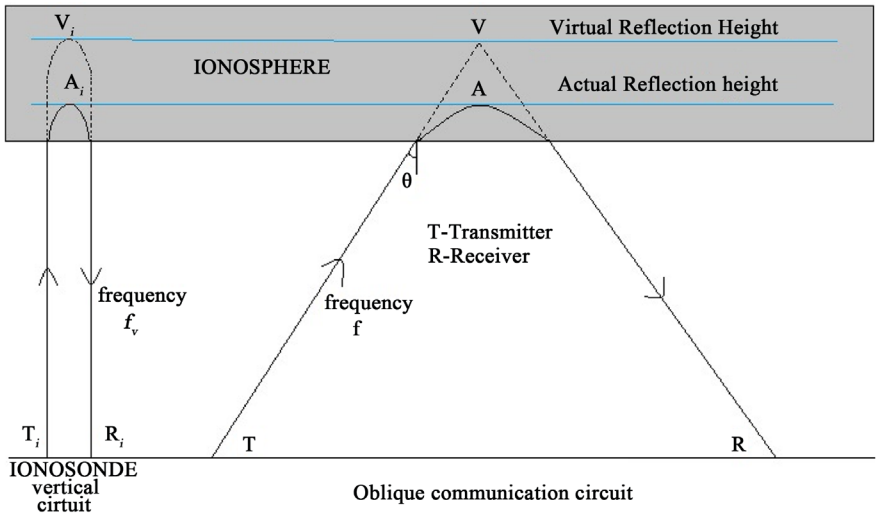

Figure 1. Schematic diagram of radio wave propagation technique through earth-ionosphere waveguide depicting the concept of critical frequency and virtual reflection height.

We found the all the chosen earthquakes are near the junction of two tectonic plates, the Nazca plate to the West and the South American plate to the East. The South American Plate is in motion, moving westward away from the Mid-Atlantic Ridge. The eastward-moving and denser Nazca Plate is sub-ducting under the western edge of the South American Plate along the Pacific coast of the continent at a rate of 77 mm per year. Subduction zones such as the South America arc are geologically complex and generate numerous earthquakes from a variety of tectonic processes that cause deformation of the western edge of South America. The Ionosonde observatory near this place is the Jicamarca Radio Observatory (JRO) (latitude 11.95˚ South, longitude 76.87˚ West). The altitude of JRO is about 520 meters above the sea level. The location of the Jicamarca observatory (blue square) and the 5 earthquakes (>6.5) in the South American region (red circle) are shown in Figure 2.

We also calculate the radius of earthquake preparation zone for these chosen earthquakes using Dobrovolsky formula [47]

$$\rho = 10^{0.43 \times M} \text{ km}$$

where ρ is the radius of the earthquake preparation zone and M is the Richter magnitude of the earthquake. We found that the distance of Jicamarca Radio Observatory from the epicenter of 5 earthquake lies within the preparation zone. The detail information of the earthquakes is given in Table 1.

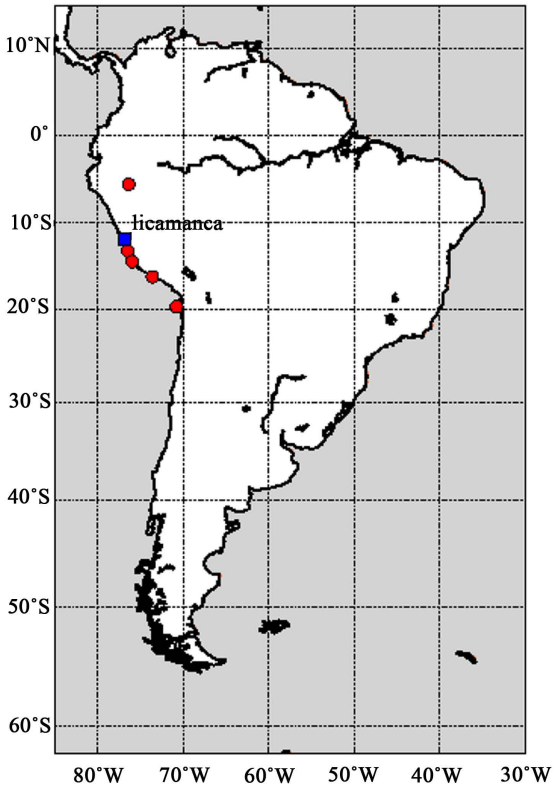

Figure 2. The location of Jicamarca Ionosonde observatory (blue square) and epicenters of five earthquakes (red circles) under consideration.

Table 1. Earthquake details.

Date	Magnitude	Lat (S)	Long (W)	Radius of preparation zone (km)	Distance from Jicamarca Radio Observatory (km)
15/08/2007	8	13.32	76.51	2754.2287	157.3
23/06/2001	8.4	16.26	73.64	4092.6065	592.4
01/04/2014	8.2	19.64	70.81	3357.3761	1073
25/09/2005	7.5	5.67	76.41	1678.8040	700.1
28/10/2011	6.9	14.52	76.01	926.8298	300.5

In Figure 3, we present a typical ionogram as obtained from the Jicamarca station. The ionogram is a six-dimensional display, with sounding frequency as the abscissa, virtual reflection height (simple conversion of time delay to range assuming propagation at 3×10^8 m/sec) as the ordinate, signal amplitude as the dot size, and echo status (Polarization, Doppler shift, and angle of arrival) mapped into 12 available distinct colors. The wave polarizations are shown as two different color groups. Firstly, the green scale, "neutral" colors showing extraordinary polarization and the red scale, "demanding attention" colors showing ordinary polarization. The angle of arrival is shown by different colors (using the "warm" scale for South and the "cold" scale for North) and the Doppler shift is indicated by the color shades. The left side of Figure shows a table of ionospheric characteristics scaled automatically by the ARTIST software [48].

The airglow intensity variation can be can mathematically represented as,

$$\text{Airglow intensity} \propto \left[f_0F_2 \right]^2 \exp\left[-\left(z - z_0 \right)/H \right]$$

Barbier [49] [50] was the first to establish a semi empirical formula for OI 6300 Å airglow emission which is given by,

$$Q_{6300} = A\left(f_0F_2 \right)^2 \exp\left[-\left(h'F - 200 \right)/H \right] + B$$

where, H is the scale height in terms of oxygen and was assumed by Barbier himself to be equal to 80 km. We only consider the variable part of this semi empirical formula and modified this equation to

$$Q_{6300} \propto \left[\left(f_0F_2 \right)^2 \exp\left(h'F/H \right) \right]$$

We name the variable quantity $\left(f_0F_2 \right)^2 \exp\left(h'F/H \right)$ as "F Parameter" and calculate this for all the five earthquakes to check possible correlations.

3. Result

We compute the F value for all the earthquakes using the f_0F_2 from the ionograms. Figure 4 shows the variation of f_0F_2 for a duration of 15 days from 18 September to 2 October 2001. The black curves are the actual values of f_0F_2 recorded as an interval of 30 minutes. So for each single day, there are 48 data points. The red curves are the average variation of f_0F_2 for the same time period

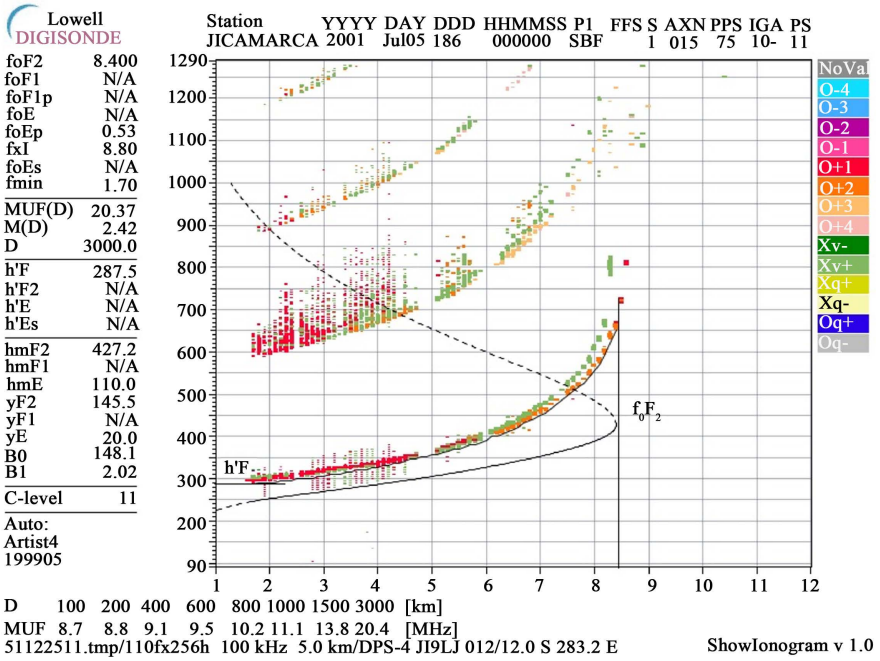

Figure 3. A typical ionogram as observed from Jicamarca Lowell Digisonde instrument (http://digisonde.com).

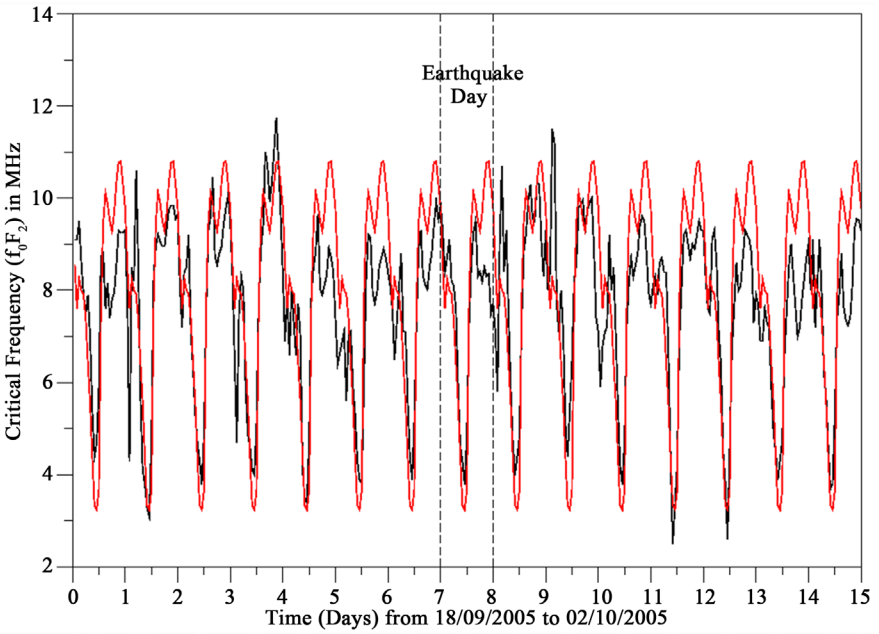

Figure 4. The variation of f_0F_2 as a function of day number around the earthquake day on 25 September, 2005. The black curves are the actual f_0F_2 variations where the red curves are the average value of f_0F_2 when there was no earthquake. There was strong earthquake on 25 September, 2005. There is an enhancement of f_0F_2, four days before the earthquake. The peak after the earthquake day is due to the major aftershocks after the main quake.

for which there were no significant seismic event. Therefore the red curve is a basic calibration of the regular variation of f_0F_2 in a seismically quiet condition.

An earthquake of Richter scale magnitude ($M = 7.5$) occurred on 25 September,

2005. It is clear from the above Figure that the value of f_0F_2 increases unusually four days before the earthquake. There is a similar enhancement of f_0F_2 just after the earthquake. After the main shock there were a series of aftershocks up to 3 to 4 days with average magnitude more than 5.5. The origin of the second peak is possibly due to these aftershocks.

We computed F parameter for all the earthquakes under consideration using the formula mentioned above. Figure 5 shows variation of F parameter as a function of time in days for a span of 21 (10 days before and after) days around the earthquake. The thick curve is the average value of F parameter. We calculate the standard deviation from the mean value and plotted the ±σ, ±2σ and ±3σ with the thick dashed, dotted-dashed and dotted curves respectively with the average value.

Figure 5 shows an enhancement of the F parameter six days before the earthquake. The zero of the X-axis represents the day of the earthquake. It is clear that the F parameter increases anomalously with an order of more than 5σ from the average value. The variation of F parameter does not follow the actual f_0F_2 variation as presented in Figure 4. There is no secondary maximum after the earthquake day. So the entire effect is pre-seismic.

In Figure 6, we present variation of F parameter for the rest of the four earthquakes in a single grid. The for graphs represents the earthquake as (a) 01/04/2014; (b) 15/08/2007; (c) 23/06/2001 and (d) 28/10/2011. We follow the same convention for calculating the σ and put the different σ level envelop with the same line style we use in Figure 5. The zero represents the earthquake day marked as E.

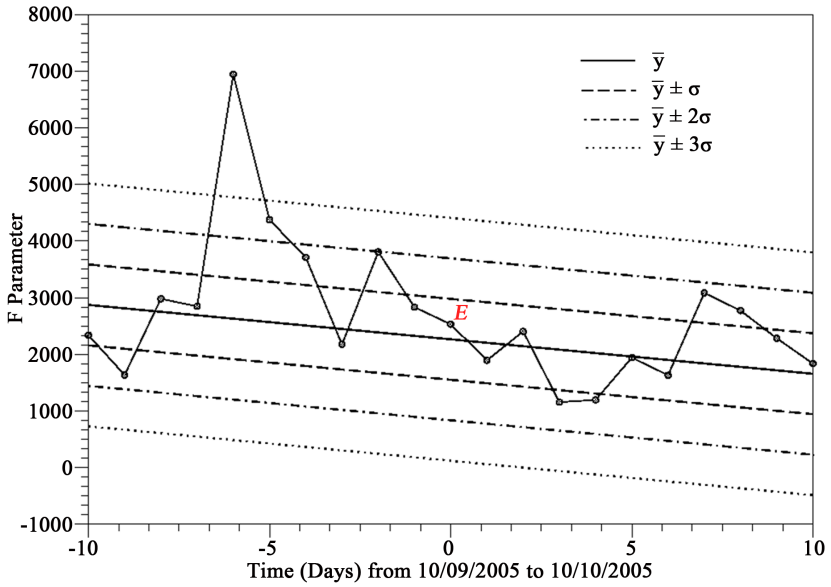

Figure 5. The variation of F parameter as a function of day number for ±10 days around the earthquake day on 25 September, 2005. The thick solid curve is the average value of the F parameter. The dashed, dotted-dashed and dotted curves are for ±σ, ±2σ and ±3σ level respectively added with the average curve. E is the day of the earthquake. F parameter shows an enhancement before the earthquake.

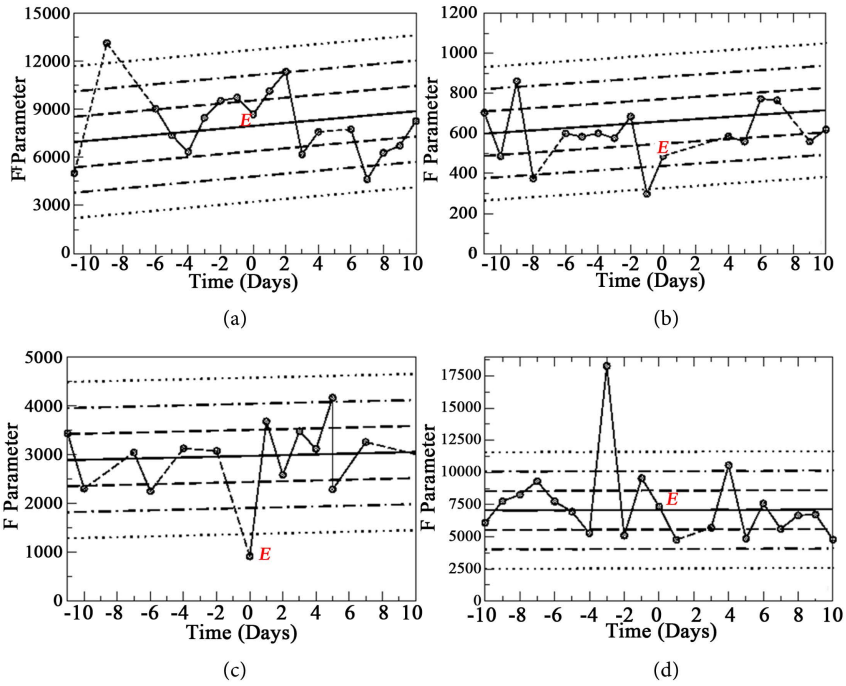

Figure 6. The variation of f 0 F 2 as a function of day number for the four earthquakes (a) 01/04/2014; (b) 15/08/2007; (c) 23/06/2001 and (d) 28/10/2011. The dashed, dotted-dashed and dotted curves are for ±σ, ±2σ and ±3σ level respectively added with the average curve. E is the day of the earthquake.

Figure 6 shows a similar enhancement of F parameter for all the cases. For (a), (b) and (d), the F parameter suffers from an enhancement on 3 to 9 days before the earthquake. For the case of 28 October, 2011 (d), the maximum is quite sharp and reaches more than 7σ level. For (a) 1 April, 2014 and (b) 15 August, 2007, the enhancement is not so sharp but crosses 3σ and 2σ level respectively. For the case of (c) 23 June, 2001, the behavior of F parameter is still anomalous but rather different. The F value becomes minimum on the day of the earthquake. Before the earthquake the F value is quite higher than that for the earthquake day but the values just cross the σ level. The value has a pre-seismic maxima on 11 days prior to the maxima but have significant secondary maxima on 2 to 5 days after the earthquake day. There are two possible reasons behind this post-seismic maxima. First, there are a series of aftershocks occurred for this earthquake. Secondly, there was another strong earthquake with Magnitude M = 7.6 occurring on 7 July, 2001. The secondary peak can be due to pre-seismic effects of the second quake as the second main shock occurs within the next 14 days. So we believe the post-seismic shocks are due to the combined effects of these two factors. To check the solar geomagnetic condition during the earthquake and its associated days we plot the geomagnetic k p index for ±7 days around the earthquake day for all the 5 earthquakes. **Figure 7** shows variation of kp index for a duration of 15 days.

It is clear from **Figure 7** that during all the earthquakes and their surrounding days, the value k p index ranges between 0 to 4.29 which implies geomagnetically

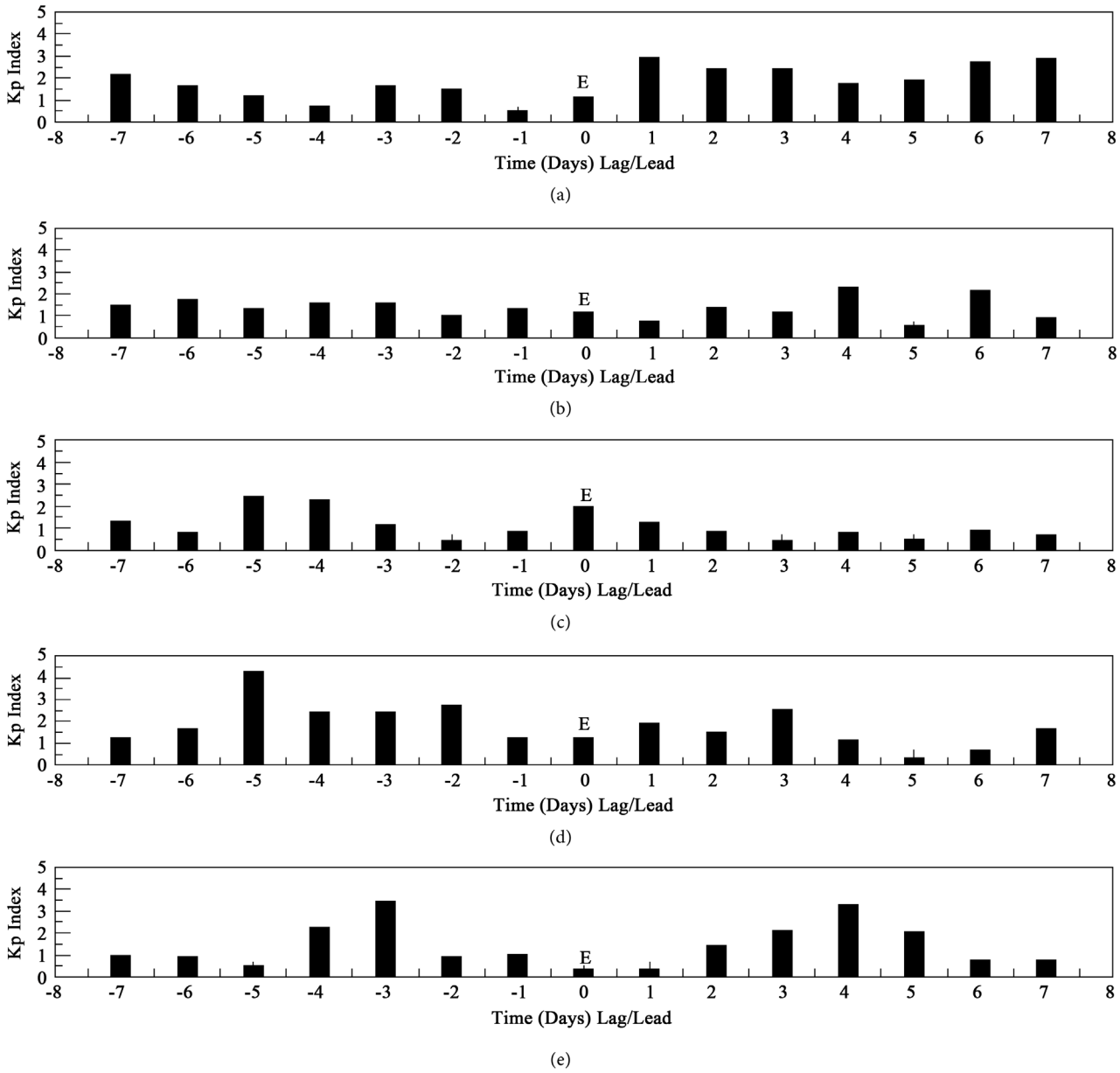

Figure 7. Variation of geomagnetic k p index on and around five earthquakes [(a) 25/09/2005; (b) 01/04/2014; (c) 15/08/2007; (d) 23/06/2001 and (e) 28/10/2011]. For all the earthquakes, kp index is below 5.

quiet condition (kp < 5). So for the signal has no perturbation due to solar geomagnetic activities and the anomaly in the signal is due to the seismic events.

4. Conclusion

The LAIC mechanism relates properties of apparently distant and distinct components of Earth system science ranging from lithosphere, lower ionospheric D-layer to upper F_2 layer. Starting from the tropospheric thermal anomalies, lower ionospheric electron density variation to upper ionospheric critical frequency modulation, LAIC takes into account a wide range of geochemical and geo-physical phenomena which could be affected simultaneously. In this paper,

we focused our study on the ionospheric F_2 layer where we observe the critical frequency variation for a span of three weeks during some strong seismic events in South America region. We compute a parameter (F) which contains the critical frequency of F_2 layer (f_0F_2) and the virtual reflection height (h') from the historic Barbier's airglow equation and study the behavior of this parameter during those earthquake days. We observe significant increase of this parameter on three to nine days prior to those seismic events. We observe the effects of the aftershocks in the direct observation of both f_0F_2 and F parameter. We also presented the geomagnetic kp indices for all the five earthquakes and found low geomagnetic condition during all the earthquakes, suggesting our assumption of LAIC mechanism. As yet, we have no clear idea of how and why exactly the lithospheric changes percolate into ionospheric changes. However, our study proves that such changes do occur. Study of physical mechanisms behind the LAIC mechanism and implementing acquired knowledge for future earthquake prediction, regular monitoring of such parameters is absolutely essential to achieve our goal. At the same time, we need to increase number of receiving stations so as to compare the anomalies from different points in order to locate the epicenter with accuracy.

Acknowledgements

The authors thank to Lowell Digisonde International, Prof. Bodo W. Reinisch and United States Geological Survey (USGS) for providing the ionogram and earthquake data respectively. S. Ghosh and S. Sasmal acknowledge Ministry of Earth Sciences (MoES) for financial support.

References

[1] Yntema, L. (1909) On the Brightness of the Sky and Total Amount of Starlight: An Experimental Study. Publications of the Kapteyn Astronomical Laboratory, Groningen, 22, 62.

[2] Elvey, C.T. (1950) Note on the Spectrum of the Airglow in the Red Region. *Astrophysical Journal*, **111**, 432-433. https://doi.org/10.1086/145278

[3] Davis, K. and Barker, D. (1965) Ionospheric Effects Observed around the Time of the Alaska Earthquake of March 1964. *Journal of Geophysical Research*, **70**, 2551-2553.

[4] Hayakawa, M. and Fujinawa, Y. (1994) Electromagnetic Phenomena Related to Earthquake Prediction. Terra Scientific Publication Company, Tokyo.

[5] Calais, E. and Minster, J.B. (1995) GPS detection of Ionospheric Perturbations Following the January 17, 1994, Northridge Earthquake. *Geophysical Research Letters*, **22**, 1045-1048. https://doi.org/10.1029/95GL00168

[6] Chmyrev, V.M., Isaev, N.V., Serebryakova, O.N., Sorokin, V.M. and Sobolev, Y.P. (1997) Small-Scale Plasma Inhomogeneities and Correlated ELF Emissions in the Ionosphere over an Earthquake Region. *Journal of Atmospheric and Solar-Terrestrial Physics*, **59**, 967-974. https://doi.org/10.1016/S1364-6826(96)00110-1

[7] Liperovsky, V.A., Pokhotelov, O.A., Liperovskaya, E.V., Parrot, M., Meister, C.V. and Alimov, O.A. (2000) Modification of Sporadic E-Layers Caused by Seismic Activity. *Surveys in Geophysics*, **21**, 449-486. https://doi.org/10.1023/A:1006711603561

[8] Liu, J.Y., Chen, Y.I., Chuo, Y.J. and Tsai, H.F. (2001) Variations of Ionospheric Total Content during the Chi-Chi Earthquake. *Geophysical Research Letters*, **28**, 1381-1386. https://doi.org/10.1029/2000GL012511

[9] Liu, J.Y., Chuo, Y.J., Pulinets, S.A., Tsai, H.F. and Zeng, X. (2002) A Study on the TEC Perturbations Prior to the Rei-Li, Chi-Chi and Chia-Yi Earthquakes. In: Hayakawa, M. and Molchanov, O.A., Eds., *Seismo-Electromagnetics*: *Lithosphere-Atmosphere-Ionosphere Coupling*, TERRAPUB, Tokyo, 297-301.

[10] Liu, J.Y., Chuo, Y.J., Shan, S.J., Tsai, Y.B., Pulinets, S.A. and Yu, S.B. (2004) Pre-Earthquake Anomalies Registered by Continuous GPS TEC Measurements. *Annales Geophysicae*, **22**, 1585-1593. https://doi.org/10.5194/angeo-22-1585-2004

[11] Liu, J.A., Tasi, Y.B., Chen, S.W., Lee, C.P., Chen, Y.C., Yen, H.Y., Chang, W.Y. and Liu, C. (2006) Giant Ionospheric Disturbances Excited by the M9.3 Sumatra Earthquake of 26 December 2004. *Geophysical Research Letters*, **33**, L02103. https://doi.org/10.1029/2005GL023963

[12] Gaivoronskaya, T.V. and Pulinets, S.A. (2002) Analysis of F_2-Layer Variability in the Areas of Seismic Activity. *IZMIRAN*, **2**, 20.

[13] Plotkin, V.V. (2003) GPS Detection of Ionospheric Perturbation before the 13 February 2001, El Salvador Earthquake. *Natural Hazards and Earth System Sciences*, **3**, 249-253. https://doi.org/10.5194/nhess-3-249-2003

[14] Afraimovich, E.L., Astafieva, E.I. and Voyeikov, S.V. (2004) Isolated Ionospheric Disturbances as Deduced from Global GPS Network. *Annales Geophysicae*, **22**, 47-62. https://doi.org/10.5194/angeo-22-47-2004

[15] Trigunait, A., Parrot, M., Pulinets, S. and Li, F. (2004) Variations of the Ionospheric Electron Density during the Bhuj Seismic Event. *Annales Geophysicae*, **22**, 4123-4131. https://doi.org/10.5194/angeo-22-4123-2004

[16] Pulinets, S.A. and Boyarchuk, K.A. (2004) Ionospheric Precursors of Earthquakes. Springer, Berlin, 315.

[17] Pulinets, S.A., Boyarchuk, K.A., Hegai, V.V. and Karelin, A.V. (2002) Conception and Model of Seismo-Ionosphere-Magnetosphere Coupling. In: Hayakawa, M. and Molchanov, O.A., Eds., *Seismo-Electromagnetics*: *Lithosphere-Atmosphere Ionosphere Coupling*, TERRAPUB, Tokyo, 353-361.

[18] Pulinets, S.A., Ouzounov, D., Ciraolo, L., Singh, R., Cervone, G., Leyva, A., Dunajecka, M., Karelin, A.V., Boyarchuk, K.A. and Kotsarenko, A. (2006) Thermal, Atmospheric and Ionospheric Anomalies around the Time of the Colima M 7.8 Earthquake of 21 January 2003. *Annales Geophysicae*, **24**, 835-849. https://doi.org/10.5194/angeo-24-835-2006

[19] Larkina, V.I., Migulin, V.V., Nalivaiko, A.V., Gershenzon, N.I., Gokhberg, M.B., Liperovsky, V.A. and Shalimov, S.L. (1983) Observation of VLF Emissions, Related with Seismic Activity, on the Intercosmos-19 Satellite. *Geomagnetism and Aeronomy*, **23**, 684-687.

[20] Zakharenkova, I.E., Shagimuratov, I.I., Krankowski, A. and Lagovsky, A.F. (2007) Precursor Phenomena Observation in the Electron Content Measurements before Great Hokkaido Earthquake of September 25, 2003, (M = 8.3). *Studia Geophysica et Geodaetica*, **51**, 267-278. https://doi.org/10.1007/s11200-007-0014-7

[21] Zakharenkova, I.E., Shagimuratov, I.I. and Krankowski, A. (2007) Features of the Ionosphere Behavior before the Kythira 2006 Earthquake. *Acta Geophysica*, **55**, 524-534. https://doi.org/10.2478/s11600-007-0031-5

[22] Zakharenkova, I.E., Shagimuratov, I.I., Tepenitzina, N.Y. and Krankowski, A. (2008) Anomalous Modification of the Ionospheric Total Electron Content Prior to the 26 September 2005 Peru Earthquake. *Journal of Atmospheric and Solar-Terrestrial Physics*, **70**, 1919-1928.

[23] Chakrabarti, S., Sasmal, S., Saha, M., Khan, R., Bhoumik, D. and Chakrabarti, S.K. (2007) Unusual Behavior of D-Region Ionization Time at 18.2 kHz during Seismically Active Days. *Indian Journal of Physics*, **81**, 531-538.

[24] Chakrabarti, S.K., Saha, M., Khan, R., Mandal, S., Acharyya, K. and Saha, R. (2005) Possible Detection of Ionospheric Disturbances during the Sumatra-Andaman Islands Earthquakes of December, 2004. *Indian Journal of Radio & Space Physics*, **34**, 314-317.

[25] Chakrabarti, S.K., Sasmal, S. and Chakrabarti, S. (2010) Ionospheric Anomaly Due to Seismic Activities Part 2: Evidence from D-Layer Preparation and Disappearance Times. *Natural Hazards and Earth System Sciences*, **10**, 1751-1757. https://doi.org/10.5194/nhess-10-1751-2010

[26] Sasmal, S. and Chakrabarti, S.K. (2009) Ionospheric Anomaly Due to Seismic Activities I: Calibration of the VLF signal of VTX 18.2 kHz Station from Kolkata and Deviation during Seismic Events. *Natural Hazards and Earth System Sciences*, **9**, 1403-1408. https://doi.org/10.5194/nhess-9-1403-2009

[27] Sasmal, S., Chakrabarti, S.K. and Ray, S. (2014) Unusual Behavior of Very Low Frequency Signal during the Earthquake at Honshu/Japan on 11 March, 2011. *Indian Journal of Physics*, **88**, 1013-1019. https://doi.org/10.1007/s12648-014-0520-8

[28] Ray, S., Chakrabarti, S.K., Mondal, S. and Sasmal, S. (2011) Correlation between Night Time VLF Amplitude Fluctuations and Effective Magnitudes of Earthquakes in Indian Sub-Continent. *Natural Hazards and Earth System Sciences*, **11**, 2699-2704. https://doi.org/10.5194/nhess-11-2699-2011

[29] Ray, S., Chakrabarti, S.K. and Sasmal, S. (2012) Precursory Effects in the Night Time VLF Signal Amplitude for the 18th Jan. 2011 Pakistan Earthquake. *Indian Journal of Physics*, **86**, 85-88. https://doi.org/10.1007/s12648-012-0014-5

[30] Molchanov, O.A., Hayakawa, M., Ondoh, T. and Kawai, E. (1998) Precursory Effects in the Subionospheric VLF Signals for the Kobe Earthquake. *Physics of the Earth and Planetary Interiors*, **105**, 239-248.

[31] Zelenova, T.I. and Legenka, A.I. (1989) Ionospheric Effects Related to the Moneron Earthquake of September 5(6) 1971, Izvestiya. *Earth Physics*, **25**, 848-853.

[32] Pulinets, S.A. (1998) Strong Earthquakes Prediction Possibility with the Help of Topside Sounding from Satellites. *Advances in Space Research*, **21**, 455-458.

[33] Ryu, K., Lee, E., Parrot, M. and Oyama, K.I. (2014) Multisatellite Observations of Enhancement of Equatorial Ionization Anomaly around Northern Sumatra Earthquake of March 2005. *Journal of Geophysical Research*, **119**, 4767-4785. https://doi.org/10.1002/2013JA019685

[34] Antselevich, M.G. (1971) The Influence of Tashkent Earthquake on the Earth's Magnetic Field and the Ionosphere. In: *Tashkent Earthquake* 26 *April* 1966, FAN Publ., 187-188.

[35] Pulinets, S.A., Legenka, A.D., Karpachev, A.T., Kochenova, N.A., Fligel, M.D., Migulin, V.V. and Oraevsky, V.N. (1991) The Earthquakes Prediction Possibility on the Base of Topside Sounding Data. *IZMIRAN*, **34**, 25.

[36] Gaivoronskaya, T.V. and Zelenova, T.I. (1991) The Effect of Seismic Activity on F_2 Layer Critical Frequencies. *Journal of Atmospheric and Terrestrial Physics*, **53**, 649-652.

[37] Depuev, V. and Zelenova, T. (1996) Electron Density Profile Changes in a Pre-Earthquake Period. *Advances in Space Research*, **18**, 115-118.

[38] Chuo, Y.J., Chen, Y.I., Liu, J.Y. and Pulinets, S.A. (2001) Ionospheric f_0F_2 Variations Prior to Strong Earthquakes in Taiwan Area. *Advances in Space Research*, **27**, 1305-1310.

[39] Pulinets, S.A., Kim, V.P., Hegai, V.V., Depuev, V.K. and Radicella, S.M. (1998) Unusual Longitude Modification of the Nighttime Midlatitude F2 Region Ionosphere in July 1980 over the Array of Tectonic Faults in the Andes Area: Observations and Interpretation. *Geophysical Research Letters*, **25**, 4143-4136. https://doi.org/10.1029/1998GL900109

[40] Pulinets, S.A., Boyarchuk, K.A., Lomonosov, A.M., Khegai, V.V. and Liu, J.Y. (2002) Ionospheric Precursors to Earthquakes: A Preliminary Analysis of the f_0F_2 Critical Frequencies at Chung-Li Ground-Based Station for Vertical Sounding of the Ionosphere (Taiwan Island). *Geomagnetism and Aeronomy*, **42**, 508-513.

[41] Liu, J.Y., Chen, Y.I., Pulinets, S.A., Tsai, Y.B. and Chuo, Y.J. (2000) Seismo Ionospheric Signatures Prior to M ≥ 6.0 Taiwan Earthquakes. *Geophysical Research Letters*, **27**, 3113-3116. https://doi.org/10.1029/2000GL011395

[42] Silina, A.S., Liperovskaya, E.V., Liperovsky, V.A. and Meister, C.V. (2001) Ionospheric Phenomena before Strong Earthquakes. *Natural Hazards*, **1**, 113-118. https://doi.org/10.5194/nhess-1-113-2001

[43] Pulinets, S.A. and Legen'ka, A.D. (2003) Spatial-Temporal Characteristics of the Large Scale Disturbances of Electron Concentration Observed in the F-Region of the Ionosphere before Strong Earthquakes. *Kosmicheskie issledovaniya* (*Cosmic Research*), **41**, 1-10. https://doi.org/10.1023/A:1024046814173

[44] Rios, V.H., Kim, V.P. and Hegai, V.V. (2004) Abnormal Perturbations in the F_2 Region Ionosphere Observed Prior to the Great San Juan Earthquake of 23 November 1977. *Advances in Space Research*, **33**, 323-327.

[45] Hobara, Y. and Parrot, M. (2005) Ionospheric Perturbations Linked to a Very Powerful Seismic Event. *Journal of Atmospheric and Solar-Terrestrial Physics*, **67**, 677-685.

[46] Liperovskaya, E.V., Meister, C.V., Pokhotelov, O.A., Parrot, M., Bogdanov, V.V. and Vasileva, N.E. (2006) On Es-Spread Effects in the Ionosphere Connected to Earthquakes. *Natural Hazards and Earth System Science*, **6**, 741-744. https://doi.org/10.5194/nhess-6-741-2006

[47] Dobrovolsky, I.R., Zubkov, S.I. and Myachkin, V.I. (1979) Estimation of the Size of Earthquake Preparation Zones. *Pageoph*, **117**, 1025-1044. https://doi.org/10.1007/BF00876083

[48] Reinisch, B.W. and Galkin, I.A. (2011) Global Ionospheric Radio Observatory (GIRO). *Earth, Planets, and Space*, **63**, 377-381. https://doi.org/10.5047/eps.2011.03.001

[49] Barbier, D. (1957) La lumiere du ciel nocturne en ete a Taamanrasset. [The Light of the Night Sky in Summer in Taamanrasset.] *Comptes Rendus de l'Académie des Sciences*, **245**, 1559-1561.

[50] Barbier, D. (1959) Recherches sur la raie 6300 de la luminescence atmospherique nocturne. [Research on the 6300 Line of Atmospheric Luminescence Nocturne.] *Annals of Geophysics*, **15**, 179-217.